

Copper Oxide Nanoparticle-Coated Quartz Sand as a Catalyst for Degradation of an Organic Dye in Water

Tal Ben-Moshe · Ishai Dror · Brian Berkowitz

Received: 15 September 2011 / Accepted: 18 January 2012 / Published online: 2 February 2012
© Springer Science+Business Media B.V. 2012

Abstract Copper oxide nanoparticles were immobilized on quartz sand and their catalytic activity for the degradation of an organic dye was investigated. The use of nanoparticles as catalysts for non photo-induced oxidation of water contaminants is relatively new. The CuO catalyst has shown promising results when suspended in free form in batch systems. Because heterogeneous catalysis is often the preferred mode of operation for application of catalytic technology, we studied the effect of immobilization of the nanoparticles on quartz sand in a flow-through system and its implication for the catalytic process. The coated sand was packed in a column and its catalytic activity for the degradation of an organic dye was investigated in a series of flow-through experiments with hydrogen peroxide as the oxidant. Control experiments with uncoated sand were also performed for comparison. The coated sand demonstrated high catalytic ability, achieving complete oxidation of the dye. During the reaction, CO₂ was produced, leading to a decrease in the water saturation in the column and reduced contact surface between the nano-CuO catalysts and the dye solution. The degradation was improved by enabling a longer residence time of the dye in the column, yielding up to 85% degradation of the dye. These results suggest that CuO nanoparticle-coated sand is an

efficient catalyst for complete degradation of the organic dye.

Keywords Nano copper oxide · Oxidation · Flow-through experiment · Heterogeneous catalysis · Lissamine green B

1 Introduction

The oxidative degradation of organic pollutants by heterogeneous catalysis is considered to be one of the most effective techniques for water remediation (Ollis 1985; Mills et al. 1993; Hoffmann et al. 1995). The oxidation in these cases is usually done by suspending catalyst powder, most commonly titanium dioxide, in an aqueous solution of the pollutant, usually in the presence of an oxidation agent such as hydrogen peroxide, and irradiating it with UV/visible light to activate the catalyst. This irradiation results in in-situ formation of active radicals such as hydroxyl or superoxide that are able, in many cases, to completely oxidize the pollutants to CO₂ and H₂O. This method was shown previously to be effective for degradation of many types of organic pollutants, including chloroform (Kormann et al. 1991), pesticides (Konstantinou et al. 2001; Pourata et al. 2009), dioxins (Choi et al. 2000) and pharmaceuticals (Achilleos et al. 2010; Yang et al. 2010), as well as for removal of inorganic pollutants such as heavy metals (Tennakone and Ketippearachchi 1995; Jung et al. 2009) and inactivation of viruses and bacteria (Watts et al. 1995; Alrousan et al. 2009).

T. Ben-Moshe · I. Dror (✉) · B. Berkowitz
Department of Environmental Sciences and Energy
Research, Weizmann Institute of Science,
Rehovot, Israel 76100
e-mail: ishai.dror@weizmann.ac.il

In a previous study, we demonstrated the use of CuO nanoparticles in free form as catalysts for the degradation of alachlor and phenanthrene with hydrogen peroxide as an oxidant (Ben-Moshe et al. 2009). We showed that the reaction is not Fenton-like as it does not utilize ions as catalysts. The nanoparticle catalyst demonstrated high catalytic efficiency for the complete mineralization of the pollutants without formation of hazardous byproducts. It has the additional advantage of not requiring any type of irradiation for its activation. To further improve the reaction and incorporate the advantages of heterogeneous catalysis, which can lead to large-scale use of this technology, it is necessary to immobilize the nanoparticles in a way that will maintain their catalytic properties. This is important for a variety of applications (e.g., chemical reactions, contaminant degradation, and alternative energy).

The catalytic properties of immobilized titanium dioxide were studied extensively in the past (El-Ekabi and Serpone 1988; Tennakone et al. 1995; Xu and Langford 1997; Naskar et al. 1998; McMurray et al. 2006; Mascolo et al. 2007; Li et al. 2008). Immobilization of CuO was also investigated (Hosseinpour et al. 2010; Lomnicki et al. 2010); however, few studies investigated the use of immobilized copper oxide for catalysis in general and the removal of organic pollutants from water in particular. Akhavan and Ghaderi (2010) demonstrated the antibacterial activity of copper oxide nanoparticles immobilized on silica thin films against *Escherichia coli* bacteria. The activity was slightly enhanced by irradiation of UV/vis light. Pande et al. (2008) investigated the catalytic activity of cation exchange resin-bound copper oxide nanoparticles for alcohol oxidation in air. These nanocomposites demonstrate superior activity to the Cu nanocomposite analog. The nanocomposites maintain their catalytic properties over ten cycles of operation. Batista et al. (2010) studied the photocatalytic degradation of CuO supported on silica for the degradation of methylene blue in a batch reactor. The catalyst demonstrated some catalytic abilities; however, to achieve considerable degradation, it was necessary to irradiate the system with UV light.

Large quantities of organic dyes are discharged to natural water systems by the textile industry during dyeing and finishing processes and by other industries such as leather, food, and printing. It is estimated that over 10,000 tons of dyes are produced each year, with an estimated 1–2% discharge in production and 1–

10% loss in use (Forgacs et al. 2004). These dyes may cause considerable environmental pollution as well as pose risks to human health. The health effects of synthetic dyes have been studied extensively (Platzek et al. 1999; Walthall and Stark 1999; Tsuda et al. 2001). Due to their stability and structural diversity, these dyes are very hard to treat by conventional methods and are usually non-biodegradable (Robinson et al. 2001; Pearce et al. 2003; Lu et al. 2009; Ali 2010). Heterogeneous photocatalysis was shown previously to be a promising method for the degradation of various organic dyes (Tayade et al. 2007; Hosseinnia et al. 2010; Bernardini et al. 2010; Guo et al. 2011).

In this study, we investigate the immobilization of copper oxide nanocatalysts on quartz sand. The catalytic activity of the coated sand is then tested in a series of flow-through experiments for the degradation of an organic dye. This system is different than common heterogeneous catalysts as it is not photo-induced and does not require any type of irradiation for activation. The immobilization allows for repeated use of the catalyst, which is necessary for large-scale application of such an approach.

2 Materials and Methods

2.1 Materials

Lissamine green B, selected as the organic dye, and copper oxide nanoparticles (30 nm) were obtained from Sigma Aldrich. Peroxide solution H_2O_2/H_2O (30%) was purchased from Frutarom. Quartz sand (Accusand, 12/20 mesh, 1.1 mm; Unimin Corp.) was used as a porous medium. Deionized water (18.2 M Ω cm) was used in all experiments.

2.2 Preparation of Coated Sand

The structure and morphology of the copper oxide nanoparticles were characterized by transmission electron microscopy (TEM) and X-ray diffraction (XRD). The BET surface area was determined by N_2 adsorption. Quartz sand was soaked in hydrochloric acid for 24 h. It was then washed repeatedly with deionized water and dried at 400°C overnight. Copper oxide nanoparticles were added, 1% by weight, to the dried sand. The mixture was shaken overnight, washed repeatedly with

water to remove unattached nanoparticles, and dried at 400°C. The final mass of attached nanoparticles was determined by digesting a sample with concentrated nitric acid, sonicating for 30 min, diluting the acid to 1%, filtering, and analyzing the concentration of the metal ions in the acid solution by inductively coupled plasma mass spectrometry (ICP-MS). The coated sand was characterized by high-resolution scanning electron microscopy (HR-SEM) and energy-dispersive x-ray spectroscopy (EDS). The samples were placed on carbon tape and sputter-coated with gold–palladium (Edwards, S150). Samples were examined using High Tension Mode Ultra 55 field emission SEM.

2.3 Batch Dye Degradation Experiments

An organic dye, lissamine green B, was chosen as a model water pollutant for the experiments because of its strong light absorption in the visible part of the spectrum, which allows continuous monitoring of the dye concentration in the solution. The chemical structure of lissamine green B is presented in Fig. 1.

The CuO nanoparticles (0.1 g) were suspended in a reactor containing 100 mL of lissamine green solution with an initial concentration of 5 mg/L. Subsequently 1 mL of H₂O₂ was added to the solution as an oxidant. The reaction mixture was stirred for 300 min. Samples of the reaction solution were taken at different times, filtered, and the dye concentration was determined by measuring the absorption at 633 nm by a Cary 100 UV–Vis spectrophotometer against a blank sample. Control experiments consisting of reaction solution of the dye with and without oxidant were performed for comparison.

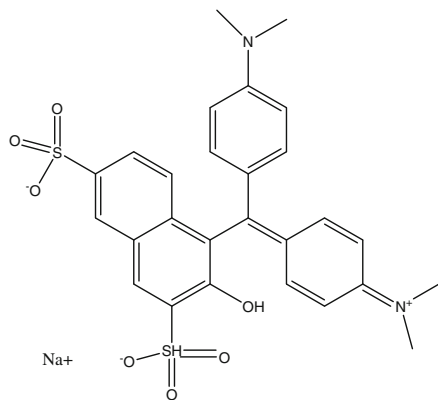


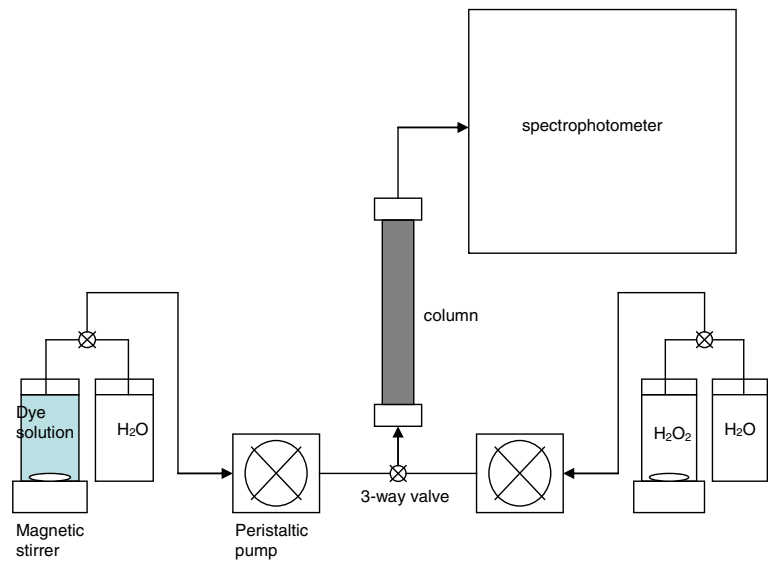
Fig. 1 Chemical structure of lissamine green B

2.4 Flow-Through Dye Degradation Experiments

The coated sand was packed into a vertical 20-cm cylindrical acrylic column with an inner diameter of 3.2 cm. The column was fully saturated with water. Water was pumped through the column and the concentration of nanoparticles at the column outlet was monitored to ensure that the particles did not leach out of the column. An aqueous solution of 5 mg/L of lissamine green B was then pumped through the column at a constant rate of 2 mL/min and the concentration at the outlet of the column was determined by measuring the absorption at 633 nm at discrete intervals. After the system was stabilized, hydrogen peroxide was added as an oxidant to the solution. The 30% solution was diluted by a factor of 100. A diagram of the experimental setup is presented in Fig. 2. Each experiment was run for 24 h after the addition of hydrogen peroxide. The weight of the column was measured at discrete intervals throughout the experiment to monitor the quantity of solution displaced by gas. The experiment was repeated with a slower flow rate of 0.5 mL/min. For this slower flow rate, reuse of the catalyst was studied. At the end of the experiment, the coated sand was washed and dried. It was then packed again in the column and the experiment was repeated. For each flow rate, an experiment with uncoated sand was also performed as a control. Each experiment was repeated twice. At the end of the experiment, the concentration of the attached nanoparticles was determined again by digesting samples from different parts of the column with acid and measuring the metal concentration by ICP-MS to evaluate the amount of nanoparticles that were lost during the experiment. The process for preparation of the samples for the ICP-MS was similar to that described in Section 2.3. The samples were also analyzed by electrospray ionization mass spectrometry (ESI-MS).

Reuse of nanoparticles in free form was tested in batch experiments. One hundred milligrams of nanoparticles were added to 10 mL of dye solution with the same initial concentration of 5 mg L⁻¹ and 0.1 mL of H₂O₂. The mixture was stirred for 2 h and filtered. The dye concentration at the end of the experiment was measured by UV–vis spectroscopy. The nanoparticles were washed and dried, and the experiment was repeated. At the end of the second experiment, the concentration of the attached nanoparticles was determined again by ICP-MS to evaluate the amount of nanoparticles that were lost.

Fig. 2 Schematic diagram of the experimental setup



The content of the gas released during the reaction was measured in a batch reactor with the same reactant concentrations. The content of the gas was measured at the end of the experiment using a gas chromatograph (GC) equipped with thermal conductivity detector and helium ionization detector. CO_2 concentrations were quantified on the basis of a calibration curve.

3 Results and Discussion

3.1 Characterization of Coated Sand

The ability of copper oxide nanoparticles to catalyze the degradation of organic dye in a flow-through system was investigated by coating the sand with nanoparticles and packing a column with the coated sand. The nanoparticles were characterized by TEM and XRD (Ben-Moshe et al. 2009). They were found to be spherical with an average size of 30 nm and surface area of $24 \text{ m}^2/\text{g}$. The mass of immobilized CuO was determined by ICP-MS to be 0.26% (w/w). The sand was characterized by HR-SEM. Images of the sand before and after the coating process, as well as coated sand at the end of the experiment, are presented in Fig. 3. The majority of the surface of the sand is coated with large aggregates of copper oxide. These aggregates were confirmed by EDS measurements to be composed of CuO . Based on visual inspection of the HR-SEM images, the sand appears to be similar before and after the flow-through experiment,

indicating that the nanoparticles are not consumed or transformed during the reaction.

3.2 Batch Dye Degradation Experiments

Batch experiments were performed to investigate the kinetics of the degradation process. The results are presented in Fig. 4. Complete degradation is achieved by the end of the experiment (5 h). The concentration of the dye decays exponentially, suggesting pseudo-first-order kinetics with respect to the dye according to the equation $C = A \exp(-kt)$, where C is the concentration of the pollutant, k is the rate constant, t is the time and A is a constant. The rate constant was calculated from the plot to be $0.01828 \pm 0.00008 \text{ min}^{-1}$. Without addition of catalyst (in the presence of H_2O_2 only), there is a linear decrease in dye concentration, but it is much slower (23% after 5 h).

3.3 Flow-Through Dye Degradation Experiments

The concentration of dye at the outlet of the column was measured by UV-vis spectroscopy. Plots of the relative concentration (concentration divided by initial concentration) vs. time are presented in Fig. 5 for two flow rates, 2 and 0.5 mL/min. Additional experiments were performed with uncoated sand as controls. The beginning of dye addition is considered the initial reaction time ($t=0$). The results are also summarized in Table 1. In the control experiment, for the higher flow rate, the relative concentration of the dye began

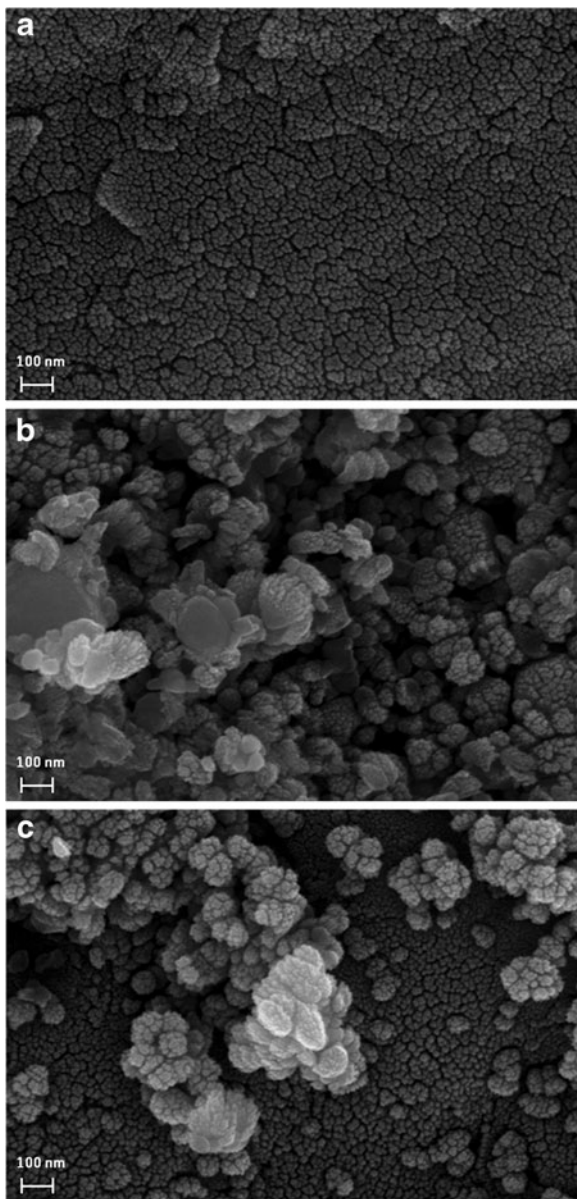


Fig. 3 HR-SEM images of non-coated sand (a) and coated sand before (b) and after (c) the experiment

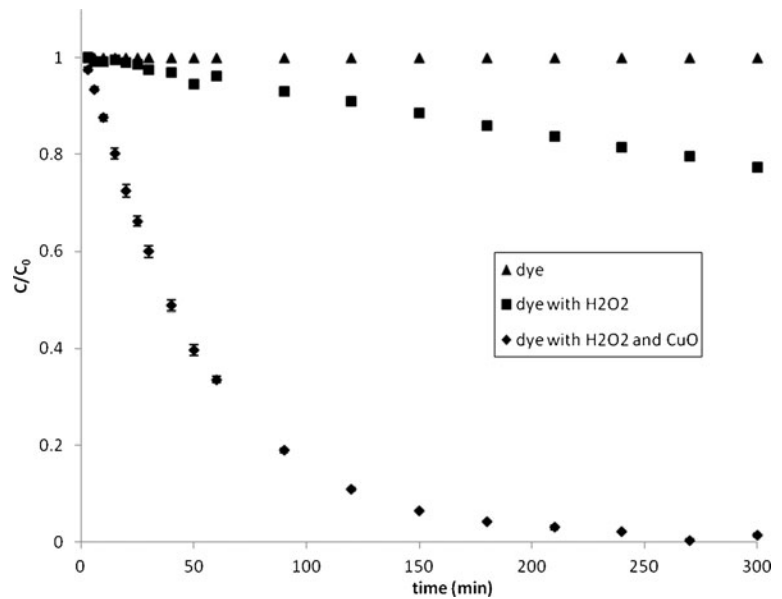
to rise after about 20 min, reaching 100% after about 60 min. Upon addition of oxidant after 1,000 min, a small decrease in concentration is evident (about 10%), suggesting degradation of the dye by the hydrogen peroxide. The concentration then rose back to 100%, and remained constant until the end of the experiment. The residence time for this flow rate was 30 min. The residence time is the time the solution spends inside the column; it is calculated by dividing

the pore volume (the volume of the column that is occupied by the solution) by the flow rate.

When the coated sand was used for the higher flow rate experiments, the initial increase in measured dye concentration at the outlet of the column was similar to the control experiment despite the expectation of higher adsorption capacity of the nanoparticles compared to the uncoated sand. In both cases, the concentration reached 100% and remained constant until the addition of hydrogen peroxide at $t=1,000$ min. This suggests a steady state in which the rate of adsorption is equal to the rate of desorption. After the addition of oxidant, rapid gas (bubbles) formation was observed inside the column. This was accompanied by a decrease in the dye concentration at the outlet of the column, reaching a value of 42% of the initial concentration, after which the concentration increased again and stabilized at 67% for the rest of the experiment. This increase can be attributed to a decrease in the pore volume due to the formation of bubbles as a result of complete degradation of the dye to carbon dioxide and water. The decrease in pore volume led to a shorter residence time of the solution in the column, so that the contact time with the catalyst was reduced and the yield of the dye degradation reaction was smaller. The formation of gas can also be attributed to release of O_2 from hydrogen peroxide degradation. The measurements of gas content are described later in this section.

Another possible explanation for the increase in relative dye concentration is a smaller catalyst area that is accessible for the dye molecules due to blocking of some of the active sites on the catalyst by the gas bubbles, making the catalysis process less efficient. The mass of CuO was determined at the end of the experiment. The nanoparticles were found to be evenly distributed inside the column. The total loss of CuO during the experiment was determined by ICP-MS to be about 2% of the CuO mass at the beginning of the experiment. To deal with the formation of bubbles and the subsequent reduction in residence time and surface area, batch experiments were performed in which the bubbles were able to leave the open reaction freely. However, many nanoparticles were found to be released from the sand to the aqueous solution during the reactions because of physical shearing among sand grains caused by magnetic or mechanical stirring.

Fig. 4 Degradation of lissamine green B in batch experiments



To improve the efficiency of the degradation process, it is necessary to increase the residence time of the solution inside the column. One way to achieve a longer residence time is to use a slower flow rate. To test this, the experiment was repeated at a slower rate of 0.5 mL/min, which leads to an increase in residence

time by a factor of four, from 30 to 120 min. In Fig. 5, a large improvement in degradation efficiency can be observed. A rise in dye concentration began after about 90 min and the concentration reached 100% after about 180 min. Upon addition of oxidant to the coated sand, a rapid decrease in dye concentration to

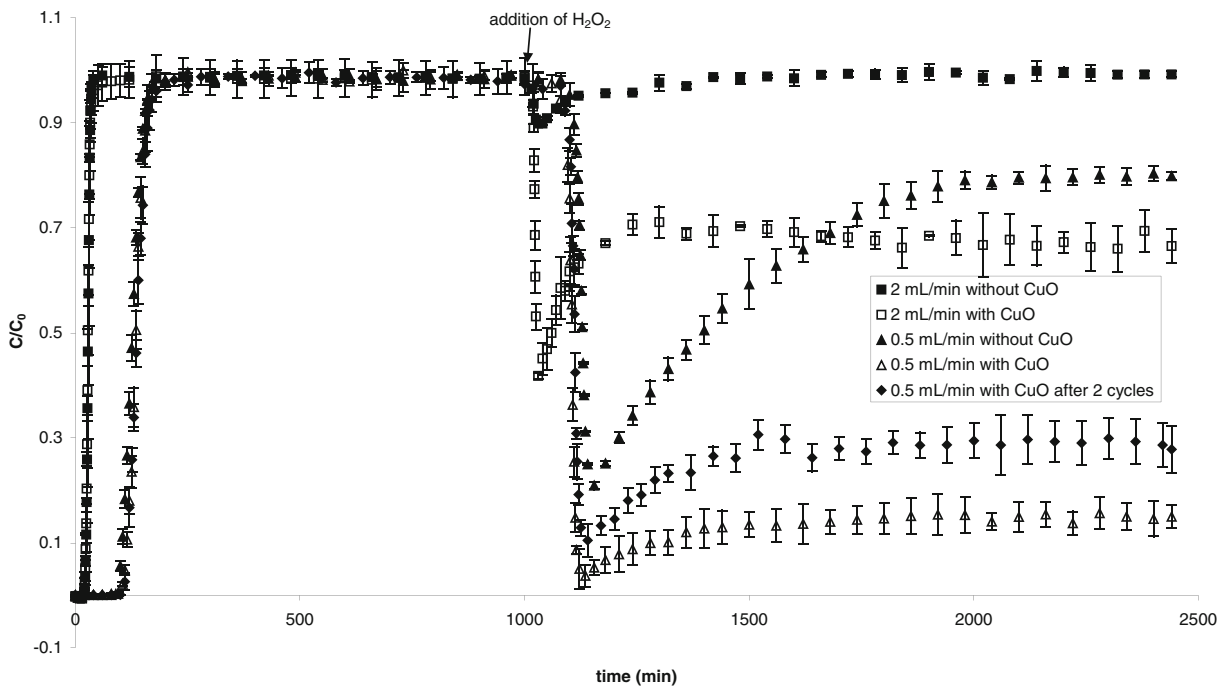


Fig. 5 Relative concentration of lissamine green B at the outlet of the column vs. time. The dye solution was added at $t=0$; hydrogen peroxide was added at $t=1,000$ min. The initial

residence times are 30 min and 120 min for 2 mL/min and 0.5 mL/min, respectively

Table 1 Summary of flow-through experiments

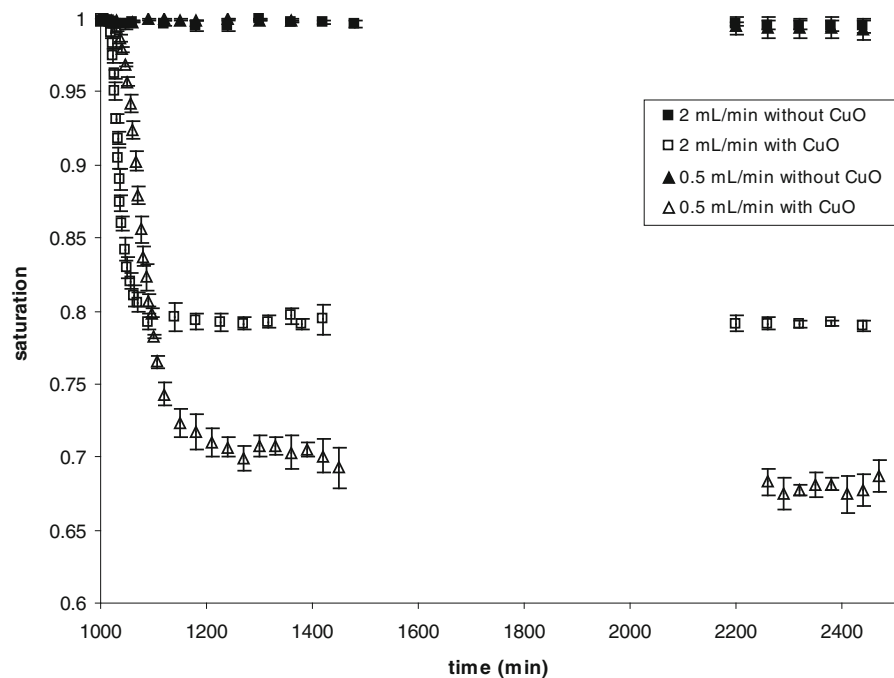
Experiment	Flow rate (mL/min)	Residence time (min)		Dye concentration (%)		Steady state saturation (%)
		Initial	Steady state	Minimum	Steady state	
Control - Fast without catalyst	2	30	30	90	100	100
Fast with catalyst	2	30	24	42	67	80
Control - Slow without catalyst	0.5	120	120	20	80	100
Slow with catalyst	0.5	120	80	4	15	67
Repacked slow with catalyst	0.5	120	–	10	29	–

about 4% (the pre-oxidant conditions) is observed (compared to 42% for the higher flow rate) followed by increase and stabilization at 15% (vs. 67% for the higher flow rate). For the non-coated sand, a rapid decrease in dye concentration is also observed (decrease to 20% and then increase and stabilization at 80%); however no gas (bubble) formation occurred.

The column weight was monitored during the experiments; these measurements were used to estimate the relative saturation of the column. Plots of the relative column saturation vs. time are presented in Fig. 6. For the coated sand, a decrease in saturation is observed upon addition of oxidant, reaching a value of 80% and 67% for the higher and lower flow rates, respectively. This change in saturation was a result of

degradation of the dye to CO₂ and water, as discussed in Section 3.4. As a result of the lower saturation, the residence times of the solution in the column are reduced from 30 and 120 min to about 24 and 80 min for the fast and slow flow rates, respectively. It is important to note that although the reaction continues for the entire duration of the experiment, the saturation reaches steady state when the rate of gas formation is equal to the rate of gas (both dissolved and in the form of visible bubbles) leaving the column. This can also be seen in the plateau in the relative concentration measurements. For the faster flow rate, the change in relative concentration between the minimum value (before the column is filled with bubbles) and the steady-state value (maximal formation of

Fig. 6 Relative column saturation vs. time, measured by changes in column weight, for flow-through experiments with and without CuO nanoparticles. No changes were observed after about 1,500 min, therefore the measurement was discontinued. Measurements were renewed toward the end of the experiment, at 2,200 min to confirm the stability of the plot



bubbles) was larger than the change expected by the relative saturation alone (see Table 1). This may be due to blocking of pores that were filled with solution by the bubbles, thus reducing the accessible surface area for reaction and the residence time, or by coating of sand grains with gas layer which reduce or prevent access to the active sites. For the slower flow rate, the change in relative concentration was smaller than the value expected by column saturation. This may indicate uneven distribution of the gas bubbles in the column, with more bubbles concentrated at the column walls, leading to a smaller change in surface area.

For the control experiments, no change in weight was observed throughout the experiment and no gas (bubbles) formation was observed despite the decrease in dye concentration upon addition of hydrogen peroxide. This indicates that without addition of catalyst, the degradation process is not complete, and carbon dioxide is not formed.

3.4 Investigation of Degradation Products

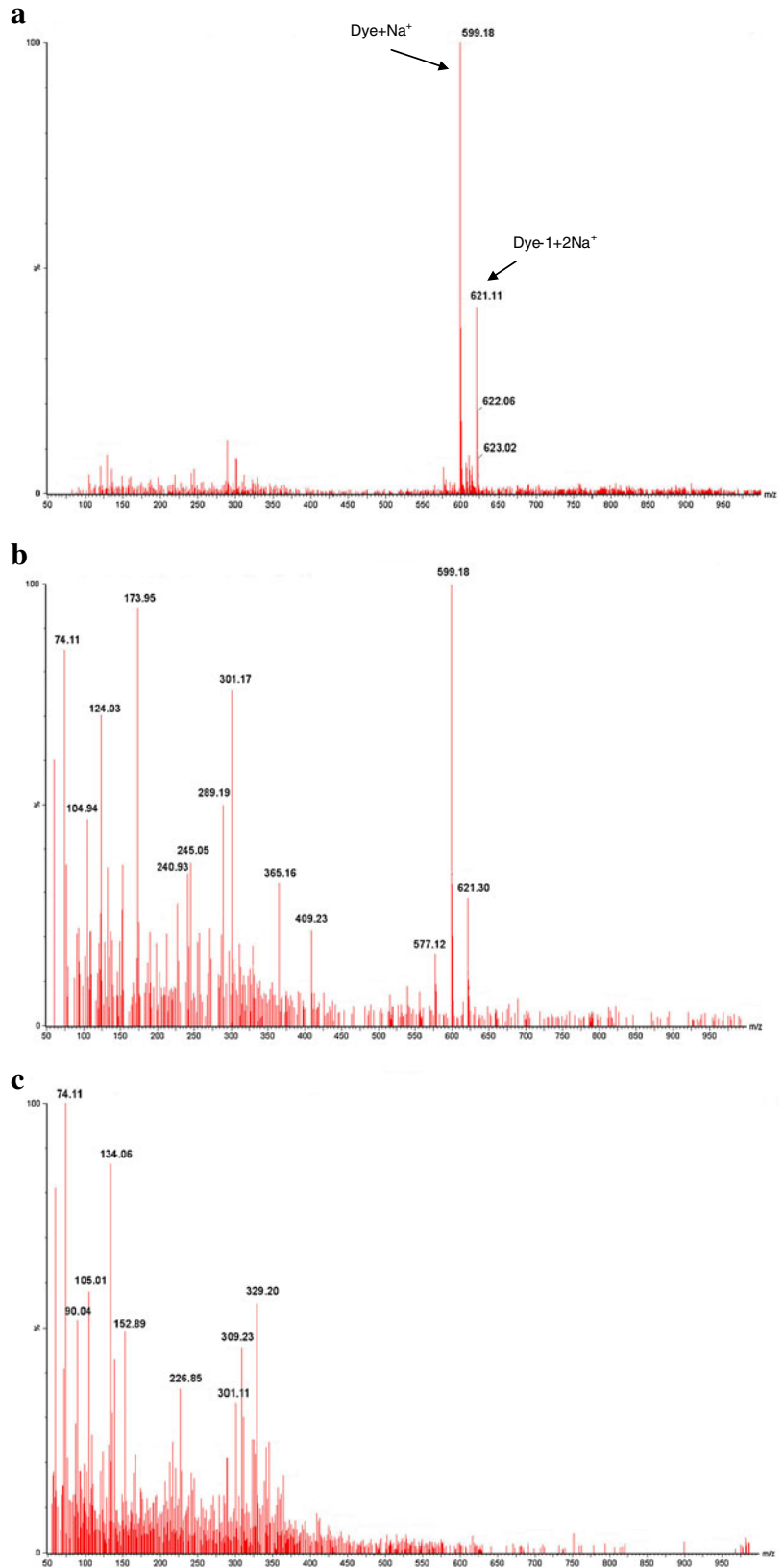
To test this hypothesis, the solution at the end of each experiment was analyzed by ESI-MS. No change in concentration of the organic carbon was measured for the samples without a catalyst. When CuO catalyst was used, a 79% decrease in concentration of organic carbon was measured. This suggests that without addition of a catalyst, incomplete degradation takes place (for the amount of dye that is reported to be transformed), while addition of catalyst leads to complete mineralization of the dye. Oxidation of the dye by hydrogen peroxide without addition of a catalyst was studied previously, and two degradation pathways were proposed (Davies and Moozyckine 2000; Moozyckine and Davies 2002); however, the reaction products were not investigated. The positive ion mode spectra of the ESI-MS measurements are presented in Fig. 7. For the dye solution, two main peaks appear at m/z 599.18, corresponding to $\text{dye} + \text{Na}^+$, and m/z 621.11, corresponding to $\text{dye} - 1 + 2\text{Na}^+$ (Fig. 7a). Upon addition of hydrogen peroxide, the original peaks are still observed; however, several additional peaks appear at lower m/z values (74.11, 124.03, 173.95, 301.17), presumably the products of incomplete oxidation (Fig. 7b). Addition of catalyst leads to the complete disappearance of the original peaks, with some formation of byproducts (m/z 74.11, 134.06, 329.20), suggesting a higher degree of degradation (Fig. 7c).

To confirm the formation of carbon dioxide in the reaction with a catalyst, the content of gas released during batch experiments was measured. Because collection of gas samples from the flow-through system is problematic, the reaction was repeated in a batch experiment in a closed vial. The gas above the aqueous solution was sampled and injected into the GC. Control experiments were also performed for comparison. The dye disappeared completely in the presence of the catalyst. For the control experiments without addition of catalyst, no change in gas content was observed. The carbon dioxide concentration did not change, suggesting that complete degradation did not take place. For the control with hydrogen peroxide, an increase in oxygen concentration was expected due to degradation of the hydrogen peroxide; however, no such change was observed during the time of the experiment. Addition of catalyst resulted in an increase in carbon dioxide and oxygen concentration. All measured concentrations were well within the detection range of the instrument. The change in carbon dioxide concentration in the headspace of the vial accounted for $61 \pm 1\%$ of the initial dye concentration. This, combined with the dissolution of CO_2 in the aqueous solution as calculated by Henry's law, accounts for all of the carbon that was initially added to the system (as the dye). The increase in oxygen concentration is attributed to degradation of hydrogen peroxide.

3.5 Investigation of Catalyst Reuse

For the slower flow rate, reuse of the coated sand catalyst was tested by washing and drying the sand at the end of the first experiment and then repacking it, and repeating the experiment. The amount of attached nanoparticles was measured again at the end of the second experiment by ICP-MS. Nanoparticle loss was $<1\%$. Upon addition of oxidant to a repacked column and repeating the experiment with the 0.5 mL/min flow rate, a decrease in relative concentration was measured. When comparing the results in Fig. 5, a substantial reduction in dye concentration was found with a minimal value of 10% followed by rise and stabilization at 30%. The efficiency of the catalyst after repacking is lower than in the first experiment. This could be either due to poisoning of the catalysts or due to mechanical problems such as loss of coated sand grains during washing, drying, and repacking. To

Fig. 7 ESI-MS spectra of: the dye solution (**a**), the solution after addition of H₂O₂ (**b**) and the solution after addition of H₂O₂ in the presence of catalyst (**c**)



test whether the nanoparticles maintain their catalytic activity (i.e., to check catalyst poisoning), batch experiments were performed with nanoparticles in free form. After the end of the first experiment, the catalyst was washed, dried, and used again. The results of two experiments were identical, with complete degradation achieved after 30 min, suggesting the nanoparticles completely maintain their catalytic activity without any catalyst-poisoning affects. It is therefore assumed that the change in degradation in the second flow-through experiment is not due to reduced catalyst activity, but rather the result of a smaller amount of available catalyst due to loss of sand grains and nanoparticles during washing, drying, and repacking of the column and loss of nanoparticles during the second experiment.

4 Conclusions

In this work, it was shown that immobilization of copper oxide nanoparticles on a porous medium can be used for catalytic degradation of organic pollutants in water. By immobilizing the nanoparticles, it is possible to easily separate them at the end of the experiment for future use. The immobilized nanoparticles demonstrated high catalytic activity for degradation of the organic dye. Disappearance of dye color was observed both with coated and uncoated sand; however, in the case of coated sand, this disappearance was accompanied by formation of gas bubbles in the column and reduced column weight, suggesting complete degradation of the dye to CO₂ and water which was also confirmed by mass balance of the CO₂ emissions. For the uncoated sand, it is assumed that incomplete degradation takes place, as confirmed by ESI-MS analyses. The efficiency of the degradation process can be improved by increasing the residence time of the solutions inside the column, for example, by using a slower flow rate. The process can be further improved by adjusting factors controlling the catalytic efficiency of the reaction, such as pH, ionic strength, and oxidant and catalyst concentrations, as done in our previous work (Ben-Moshe et al. 2009) for the degradation of alachlor and phenanthrene in batch systems.

Acknowledgments The financial support of the Gurwin Fund and the Brita Fund is gratefully acknowledged. We thank Dr. Arye Tishbee and Riri Kramer for conducting ESI-MS analyses

and Dr. Elena Kartvelishvily for conducting SEM measurements. Electron microscopy was performed in the Irving and Cherna Moscowitz Center for Nano and Bio-nano Imaging of the Weizmann Institute. BB holds the Sam Zuckerberg Professorial Chair in Hydrology.

References

- Achilleos, A., Hapeshi, E., Xekoukoulotakis, N. P., Mantzavinos, D., & Fatta-Kassinos, D. (2010). UV-A and solar photodegradation of ibuprofen and carbamazepine catalyzed by TiO₂. *Separation Science and Technology*, 45(11), 1564–1570.
- Akhavan, O., & Ghaderi, E. (2010). Cu and CuO nanoparticles immobilized by silica thin films as antibacterial materials and photocatalysts. *Surface and Coating Technology*, 205(1), 219–223.
- Ali, H. (2010). Biodegradation of synthetic dyes—A review. *Water, Air, and Soil Pollution*, 213(1–4), 251–273.
- Alroushan, D. M. A., Dunlop, P. S. M., McMurray, T. A., & Byrne, J. A. (2009). Photocatalytic inactivation of *E. coli* in surface water using immobilized nanoparticle TiO₂ films. *Water Research*, 43(1), 47–54.
- Batista, A. P. L., Carvalho, H. W. P., Luz, G. H. P., Martins, P. F. Q., Goncalves, M., & Oliveira, L. C. A. (2010). Preparation of CuO/SiO₂ and photocatalytic activity by degradation of methylene blue. *Environmental Chemistry Letters*, 8(1), 63–67.
- Ben-Moshe, T., Dror, I., & Berkowitz, B. (2009). Oxidation of organic pollutants in aqueous solutions by nanosized copper oxide catalysts. *Applied Catalysis B: Environmental*, 85(3–4), 207–211.
- Bernardini, C., Cappelletti, G., Dozzi, M. V., & Selli, E. (2010). Photocatalytic degradation of organic molecules in water: Photoactivity and reaction paths in relation to TiO₂ particles features. *Journal of Photochemistry and Photobiology, A: Chemistry*, 211(2–3), 185–192.
- Choi, W., Hong, S. J., Chang, Y. S., & Cho, Y. (2000). Photocatalytic degradation of polychlorinated dibenzo-p-dioxins on TiO₂ film under UV or solar light irradiation. *Environmental Science and Technology*, 34(22), 4810–4815.
- Davies, D. M., & Moozyckine, A. U. (2000). Kinetics and mechanism of the bleaching of a triarylmethane dye by hydrogen peroxide and water: Evidence for intramolecular base catalysis. *Journal of the Chemical Society, Perkin Transactions*, 2(7), 1495–1503.
- El-Ekabi, H., & Serpone, N. (1988). Kinetics studies in heterogeneous photocatalysis. I. Photocatalytic degradation of chlorinated phenols in aerated aqueous solutions over titania supported on a glass matrix. *Journal of Physical Chemistry*, 92(20), 5726–5731.
- Forgacs, E., Cserhati, T., & Oros, G. (2004). Removal of synthetic dyes from wastewaters: A review. *Environment International*, 30(7), 953–971.
- Guo, C., Xu, J., He, Y., Zhang, Y., & Wang, Y. (2011). Photodegradation of rhodamine B and methyl orange over one-dimensional TiO₂ catalysts under simulated solar irradiation. *Applied Surface Science*, 257(8), 3798–3803.

- Hoffmann, M. R., Martin, S. T., Choi, W., & Bahnemann, D. W. (1995). Environmental applications of semiconductor photocatalysis. *Chemical Reviews*, 95(1), 69–96.
- Hosseinnia, A., Keyanpour-Rad, M., & Pazouki, M. (2010). Photo-catalytic degradation of organic dyes with different chromophores by synthesized nanosize TiO₂ particles. *World Applied Sciences Journal*, 8(11), 1327–1332.
- Hosseinpour, M., Ahmadi, S. J., Mousavand, T., & Outokesh, M. (2010). Production of granulated-copper oxide nanoparticles for catalytic application. *Journal of Materials Research*, 25(10), 2025–2034.
- Jung, J. T., Choi, J. Y., Chung, J., Lee, Y. W., & Kim, J. O. (2009). UV/TiO₂ and UV/TiO₂/chemical oxidant processes for the removal of humic acid, Cr and Cu in aqueous TiO₂ suspensions. *Environmental Technology*, 30(3), 225–232.
- Konstantinou, I. K., Sakellarides, T. M., Sakkas, V. A., & Albanis, T. A. (2001). Photocatalytic degradation of selected s-triazine herbicides and organophosphorus insecticides over aqueous TiO₂ suspensions. *Environmental Science and Technology*, 35(2), 398–405.
- Kormann, C., Bahnemann, D. W., & Hoffmann, M. R. (1991). Photolysis of chloroform and other organic molecules in aqueous titanium dioxide suspensions. *Environmental Science and Technology*, 25(3), 494–500.
- Li, F., Sun, S., & Jiang, Y. (2008). Photodegradation of an azo dye using immobilized nanoparticles of TiO₂ supported by natural porous mineral. *Journal of Hazardous Materials*, 152(3), 1037–1044.
- Lomnicki, S. M., Wu, H., Osborne, S. N., Pruetz, J. M., McCarley, R. L., Poliakov, E., & Dellinger, B. (2010). Size-selective synthesis of immobilized copper oxide nanoclusters on silica. *Materials Science and Engineering*, 175(2), 136–142.
- Lu, L., Zhao, M., Liang, S. C., Zhao, L. Y., Li, D. B., & Zhang, B. B. (2009). Production and synthetic dyes decolorization capacity of a recombinant laccase from *Pichia pastoris*. *Journal of Applied Microbiology*, 107(4), 1149–1156.
- Mascolo, G., Comparelli, R., Curry, M. L., Lovecchio, G., & Agostiano, A. (2007). Photocatalytic degradation of methyl red by TiO₂: Comparison of the efficiency of immobilized nanoparticles versus conventional suspended catalyst. *Journal of Hazardous Materials*, 142(1–2), 130–137.
- McMurray, T. A., Dunlop, P. S. M., & Byrne, J. A. (2006). The photocatalytic degradation of atrazine on nanoparticulate TiO₂ films. *Journal of Photochemistry and Photobiology, A: Chemistry*, 182(1), 43–51.
- Mills, A., Davies, R. H., & Worsley, D. (1993). Water purification by semiconductor photocatalysis. *Chemical Society Reviews*, 22(6), 417–425.
- Moozyckine, A. U., & Davies, D. M. (2002). Green S as a prototype for an environmentally-degradable dye: the concept of a 'green dye' in future green chemistry. *Green Chemistry*, 4(5), 452–458.
- Naskar, S., Pillay, S. A., & Chandra, M. (1998). Photocatalytic degradation of organic dyes in aqueous solution with TiO₂ nanoparticles immobilized on foamed polyethylene sheet. *Journal of Photochemistry and Photobiology, A: Chemistry*, 113(3), 257–264.
- Ollis, D. F. (1985). Contaminant degradation in water. *Environmental Science and Technology*, 19(6), 480–484.
- Pande, S., Saha, A., Jana, S., Sarkar, S., Basu, M., Pradhan, M., Sinha, A. K., Saha, S., Pal, A., & Pal, T. (2008). Resin-immobilized CuO and Cu nanocomposites for alcohol oxidation. *Organic Letters*, 10(22), 5179–5181.
- Pearce, C. I., Lloyd, J. R., & Guthrie, J. T. (2003). The removal of colour from textile wastewater using whole bacterial cells: A review. *Dyes and Pigments*, 58(3), 179–196.
- Platzek, T., Lang, C., Grohmann, G., Gi, U. S., & Baltes, W. (1999). Formation of a carcinogenic aromatic amine from an azo dye by human skin bacteria in vitro. *Human & Experimental Toxicology*, 18(9), 552–559.
- Pourata, R., Khataee, A. R., Aber, S., & Daneshvar, N. (2009). Removal of the herbicide Bentazon from contaminated water in the presence of synthesized nanocrystalline TiO₂ powders under irradiation of UV-C light. *Desalination*, 249(1), 301–307.
- Robinson, T., McMullan, G., Merchant, R., & Nigam, P. (2001). Remediation of dyes in textile effluent: A critical review on current treatment technologies with a proposed alternative. *Bioresource Technology*, 77(3), 247–255.
- Tayade, R. J., Suroli, P. K., Kulkarni, R. G., & Jarsa, R. V. (2007). Photocatalytic degradation of dyes and organic contaminants in water using nanocrystalline anatase and rutile TiO₂. *Science and Technology of Advanced Materials*, 8(6), 455–462.
- Tennakone, K., & Ketiprachchi, U. S. (1995). Photocatalytic method for removal of mercury from contaminated water. *Applied Catalysis B: Environmental*, 5(4), 343–349.
- Tennakone, K., Tilakaratne, C. T. K., & Kottegodla, I. R. M. (1995). Photocatalytic degradation of organic contaminants in water with TiO₂ supported on polythene films. *Journal of Photochemistry and Photobiology, A: Chemistry*, 87(2), 177–179.
- Tsuda, S., Murakami, M., Matsusaka, N., Kano, K., Taniguchi, K., & Sasaki, Y. F. (2001). DNA damage induced by red food dyes orally administered to pregnant and male mice. *Toxicological Sciences*, 61(1), 92–99.
- Walthall, W. K., & Stark, J. D. (1999). The acute and chronic toxicity of two xanthene dyes, fluorescein sodium salt and phloxine B, to *Daphnia pulex*. *Environmental Pollution*, 104(2), 207–215.
- Watts, R. J., Kong, S., Orr, M. P., Miller, G. C., & Henry, B. E. (1995). Photocatalytic inactivation of coliform bacteria and viruses in secondary wastewater effluent. *Water Research*, 29(1), 95–100.
- Xu, Y., & Langford, C. H. (1997). Photoactivity of titanium dioxide supported on MCM41, zeolite X, and zeolite Y. *The Journal of Physical Chemistry. B*, 101(16), 3115–3121.
- Yang, H., An, T., Li, G., Song, W., Cooper, W. J., Luo, H., & Guo, X. (2010). Photocatalytic degradation kinetics and mechanism of environmental pharmaceuticals in aqueous suspension of TiO₂: A case of β -blockers. *Journal of Hazardous Materials*, 179(1–3), 834–839.